Available online at www.sciencedirect.com
SCIENCE DIRECT®
Chemical Physics Letters 401 (2005) 62–67
CHEMICAL PHYSICS LETTERS
www.elsevier.com/locate/cplett

OD ESR detection of the radical anions of cyclic nitrones in liquid solutions

M.M. Barlukova [a,b,*], N.P. Gritsan [a,b], V.A. Bagryansky [a,b], V.F. Starichenko [c], I.A. Grigor'ev [b,c], Yu.N. Molin [a]

[a] *Institute of Chemical Kinetics and Combustion, 3, Institutskaya Str., 630090 Novosibirsk, Russia*
[b] *Novosibirsk State University, 630090 Novosibirsk, Russia*
[c] *N.N. Vorozhtsov Novosibirsk Institute of Organic Chemistry, 630090 Novosibirsk, Russia*

Received 9 July 2004; in final form 29 October 2004

Abstract

The radical anions of five-membered cyclic nitrone spin traps, 3,3,5,5-tetramethyl-1-pyrroline-1-oxide and 1,2,2,5,5-pentamethyl-3-imidazoline-3-oxide, formed under radiolysis of liquid squalane solutions at 250–268 K, were registered by the method of optically detected ESR, and the hfc constants and *g*-values of the radical anions were determined. The hfc constants of these radical anions were predicted by DFT calculations and were found to be in quantitative agreement with experiment. It was demonstrated that radical anions of the five-membered cyclic nitrones have non-planar geometry with the spin density localized in the C═N─O fragment.

1. Introduction

Nitrones are widely used as spin traps to validate participation of free radicals in different chemical and biochemical reactions [1]. This application is based on the ability of the nitrone group (**1**) to add short-lived free radicals to form stable nitroxide radicals (**2**) (see Scheme 1).

In 1986, Chandra and Symons [2] reported on the ESR spectrum of the radical cation (RC) of 5,5-dimethyl-1-pyrroline-1-oxide in the Freon matrix at 77 K. They revealed the ability of this radical cation to react with nucleophiles, forming a nitroxide radical. This process, confirmed by further investigations, e.g. [3–5], was called the 'inverted spin trapping' [6]. It was assumed [4,7–10] that nitroxide radicals could also be formed via the mechanism involving the radical anions (RAs) of spin traps. Obviously, alternative channels of the nitroxide radical formation must be taken into account in the interpretation of the spin traping experiments.

While a considerable attention was paid to the study of the processes involving RCs [3–5,10–14], much less is known about RAs of nitrone spin traps, probably, due to a lower stability of these species as compared with the RCs of nitrones. To the best of our knowledge there is only one communication [15] about an ESR spectrum of RA detected during electrochemical reduction of dinitrone.

In the present Letter, the radical anions of cyclic nitrones have been detected for the first time by the method of optically detected ESR (OD ESR).

2. Experimental and computational details

2.1. OD ESR experiments

The OD ESR method is applied to detect spin-correlated radical ion pairs formed in dilute solutions of elec-

* Corresponding author. Fax: +7 3832 342350.
E-mail address: barlukova@ns.kinetics.nsc.ru (M.M. Barlukova).

0009-2614/$ - see front matter © 2004 Elsevier B.V. All rights reserved.
doi:10.1016/j.cplett.2004.11.024

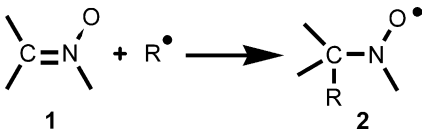

Scheme 1. Spin trapping reaction.

tron acceptor A and electron donor D upon continuous ionizing irradiation [16]. The radical ion pairs $A^{\bullet -}/D^{\bullet +}$, produced in the non-polar solutions in the singlet spin state, can recombine to form singlet excited molecules, which can emit light.

$$D^{\bullet +} + A^{\bullet -} \rightarrow D^{*} + A(\text{or } D + A^{*}) \rightarrow D + A + h\nu$$

In a magnetic field of the OD ESR spectrometer, the hyperfine coupling (hfc) and the difference in the *g*-values of the radicals cause the singlet–triplet $S–T_0$ transitions in a pair. Under the resonance mw pumping, the ESR-transitions occur between the T_0 and T_+ T_- states of the pair. This leads to an additional decrease in the population of singlet level and as a consequence to a drop in fluorescence intensity, thus giving rise to the OD ESR signal. When mw magnetic field is much less than the width of the ESR spectrum, the OD ESR spectrum is the superposition of ESR spectra of both recombining radical ions with equal integral intensity [16]. Therefore, the OD ESR method, being sensitive selectively to radical ion pairs, allows detecting spectra of short-lived (with lifetimes up to 10^{-8} s) RCs and RAs in liquid solutions.

The OD ESR spectrometer is based on an ER-200D Bruker ESR-spectrometer supplied with a source of ionizing radiation (X-ray tube) and photomultiplier (FEU-130, Russia) to measure fluorescence intensity [17]. As a detecting device, the SR810DSP lock-in amplifier (USA) was used. The OD ESR spectra were recorded at a mw-power of 5 W and a modulation amplitude of 0.36 mT. To determine hfc constants, the recorded OD ESR spectra were simulated using the 'WinSim-2002' program. The *g*-values were determined from the shift of the analyzed spectrum relative to the signal of the *para*-terphenyl-d_{14} RA for which $g = 2.0027$ [18].

2.2. Materials

The cyclic nitrone 3,3,5,5-tetramethyl-1-pyrroline-1-oxide (TMPO) was kindly provided by prof. V.A. Reznikov (NIOC, Novosibirsk), and 1,2,2,4,5,5-pentamethyl-3-imidazoline-3-oxide (PMIO) was synthesized according to [19]. The structures of both cyclic nitrones are presented in Fig. 1.

There are no data on the electron affinities of TMPO and PMIO. However, it can be assumed from the data on similar compounds, that TMPO and PMIO can form RAs in alkane solutions. To record the OD ESR spectra of a radical anion, the electron donor with a high quantum yield of fluorescence was added to the solution. In this case, the spectrum obtained would belong to the pair $D^{\bullet +}$/(cyclic nitrone)$^{\bullet -}$.

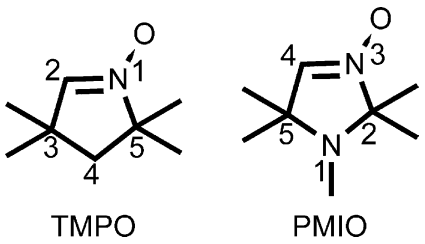

Fig. 1. Structures of the studied compounds.

In the present work, we used as positive charge traps durene $C_{10}H_{14}$ (>99%, Fluka, EA<0.048 eV [20], IE = 8.07 eV [21]), deuterated toluene C_7D_8 (98%, Aldrich, IE = 8.83 eV [22]), or tetramethyl-*para*-phenylendiamine (TMPD) (98%, Aldrich, IE = 6.1 eV [23]). We also used *para*-terphenyl-d_{14} (*p*-TP) (99%, Aldrich) characterized by the fluorescence quantum yield close to unity, as emitting probe. All the luminophors were used as received.

As solvent, we used squalane (2,6,10,15,19,23-hexamethyltetracosane, 99%, Fluka). To increase the geminate recombination time and thus increase the OD ESR signal-to-noise ratio, the samples were cooled down to temperatures of 255–268 K. The solvent was purified on a chromatographic column with alumina activated with silver nitrate (10%). The solvent purity was monitored by its UV absorption spectrum. The optical density of the fraction used was equal to 1 at a wavelength of 210 nm in a 1 cm layer. Solutions were degassed by repeated freeze–pump–thaw cycles (pump to $\sim 10^{-3}$ Torr) and sealed off in thin-walled quartz cuvettes.

2.3. Quantum chemical calculations

The geometries of the RAs were optimized using both ab initio (UMP2/6-311G(p,d)) and semi-empirical (UPM3 [24]) quantum chemical methods as well as density functional theory at the hybrid UB3LYP level [25,26] with the 6-311G(p,d) basis set using the GAUSSIAN 98 suit of programs [27]. The hfc constants were calculated using B3LYP method with 6-31G* and EPR-II [28,31] basis sets at geometries optimized as described above.

The energy (ΔE) released during recombination of radical ion pairs $A^{\bullet -}/D^{\bullet +}$ and accessible for the electronic excitation of one of the partners was estimated as the difference in the total electronic energies of the radical ion pair (taking into account solvation energy and the Coulombic interaction of ions) and the resulting molecules.

$$A^{\bullet -} + D^{\bullet +} \rightarrow A + D + \Delta E \quad (1)$$

Here it was assumed that during electron transfer, the geometrical structure had no time to relax and a neutral molecule exhibited the radical ion geometry. The electronic energies of radical ions and neutral molecules were calculated at the B3LYP/6-311G(p,d) level. The free energies of solvation of all the species were calculated using the polarized continuum model (PCM or Tomashi model) [30,31] as implemented in the GAUSSIAN 98 suit of programs. Calculations were performed for a non-polar solvent (heptane) whose properties are similar to those of squalane used in our experiments. The energy of the electrostatic interaction E_{el} of RC and RA in the radical ion pairs was estimated according to the Eq. (2)

$$E_{el} = -e^2/\epsilon R, \quad (2)$$

where R is the distance between the cation and the anion.

3. Results and discussion

For more reliable identification of the RAs of nitrones, we used three different hole traps (TMPD, deuterotoluene, and durene) as luminophors. For durene and per-deuterotoluene, the recorded signals appeared to be rather weak due to the relatively low quantum yield of fluorescence of these substances. However, after addition to a solution of a small amount of *p*-TP (8×10^{-5} M), the signal-to-noise ratio increased several times while the spectrum shape remained unchanged. It was assumed that under these conditions, the contribution of *p*-TP radical ions to the OD ESR spectrum was negligible. An increase in the signal intensity can be attributed to the electronic excitation transfer from durene or per-deuterotoluene to the *p*-TP molecules whose fluorescence quantum yield is much higher and the fluorescence spectrum is noticeably shifted toward longer wavelengths, where the photomultiplier spectral sensitivity is much higher.

3.1. Tetramethyl-para-phenylenediamine as hole trap

TMPD is characterized by a high fluorescence quantum yield, which allows us to record high quality OD ESR spectra without adding *p*-TP as an emitting probe. A hyperfine splitting in the ESR spectrum of TMPD RC is determined by the interaction with two nitrogen nuclei $a_N(2NH_2) = 0.705$ mT and protons of four methyl groups $a_H(4CH_3) = 0.677$ mT and protons of two amine groups $a_H(2NH_2) = 0.199$ mT [32]. Under our experimental conditions, the spectrum of this RC is a broad unresolved single line. The OD ESR spectrum of the squalane solution containing 10^{-2} M of both TMPO and TMPD is presented in Fig. 2. This spectrum is a superposition of the unresolved line of $TMPD^{\bullet+}$ and poorly resolved six-line multiplet of $TMPO^{\bullet-}$. The best fit (smooth) for the experimental spectrum gives for $TMPO^{\bullet-}$ $g = 2.0038 \pm 0.0002$, $a_N(NO) = 1.20$ mT, and $a_H(CH) = 0.53$ mT. The integral intensities of the $TMPO^{\bullet-}$ and $TMPD^{\bullet+}$ spectra are equal within the experimental accuracy.

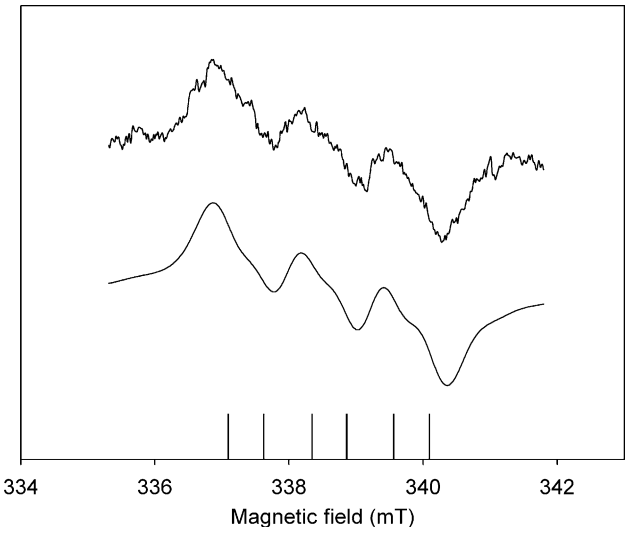

Fig. 2. OD ESR spectrum of squalane solution of 10^{-2} M TMPD + 10^{-2} M TMPO at $T = 262$ K. Smooth curve is modelling of the spectrum with parameters: $a_N(2NH_2) = 0.71$ mT, $a_H(4CH_3) = 0.68$ mT, $a_H(2NH_2) = 0.2$ mT for TMPD RC; $a_N(NO) = 1.2$ mT, $a_H(CH) = 0.53$ mT for TMPO RA, the individual line width is 0.27 mT.

We failed to detect OD ESR signal in the PMIO/TMPD solution. We propose that the energy released upon recombination of the $TMPD^{\bullet+}/PMIO^{\bullet-}$ pairs is insufficient for the formation of TMPD molecule in the singlet excited state. Indeed, the estimations according to Eq. (1) suggest that the energy ΔE released upon recombination of the $TMPD^{\bullet+}/PMIO^{\bullet-}$ pair is 0.1–0.3 eV lower than for the case of the $TMPD^{\bullet+}/TMPO^{\bullet-}$ pair recombination (Table 1).

3.2. Deuterotoluene as a hole trap

Fig. 3 displays the spectra recorded in the solution containing deuterotoluene as a hole-trap. Note, that its RC has a relatively narrow spectrum, which superimposes the central part of the spectra of TMPO and PMIO RAs.

Table 1
Estimation of the energy (ΔE), released upon recombination of radical ion pairs (R – distance between ions)

Radical ion pair	ΔE (R = 5 Å) (eV)	ΔE (R = 10 Å) (eV)
$TMPO^{-\bullet}/TMPD^{+\bullet}$	2.6	3.2
$PMIO^{-\bullet}/TMPD^{+\bullet}$	2.3	3.1
$TMPO^{-\bullet}/p\text{-}TP^{+\bullet}$	4.0	4.8
$PMIO^{-\bullet}/p\text{-}TP^{+\bullet}$	3.9	4.6
$p\text{-}TP^{-\bullet}/p\text{-}TP^{+\bullet}$	3.8	4.6

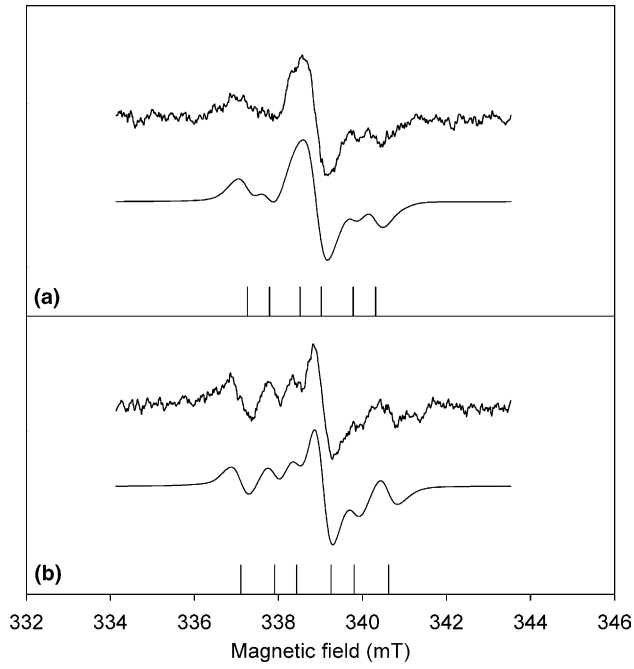

Fig. 3. OD ESR spectra of squalane solutions of: (a) 8×10^{-5} M *p*-TP + 10^{-2} M toluene-d_8 + 10^{-2} M TMPO at $T = 268$ K; (b) 8×10^{-5} M *p*-TP + 10^{-2} M toluene-d_8 + 10^{-2} M PMIO at $T = 255$ K. Smooth curves are modelling of the spectra with parameters: $a_D(CD_3) = 0.18$ mT, $a_D(p) = 0.28$ mT for toluene-d_8 RC; $a_N(NO) = 1.23$ mT, $a_H(CH) = 0.46$ mT for TMPO RA; $a_N(NO) = 1.32$ mT, $a_H(CH) = 0.9$ mT for PMIO RA, the individual line widths are 0.25 mT (spectrum a) and 0.29 mT (spectrum b).

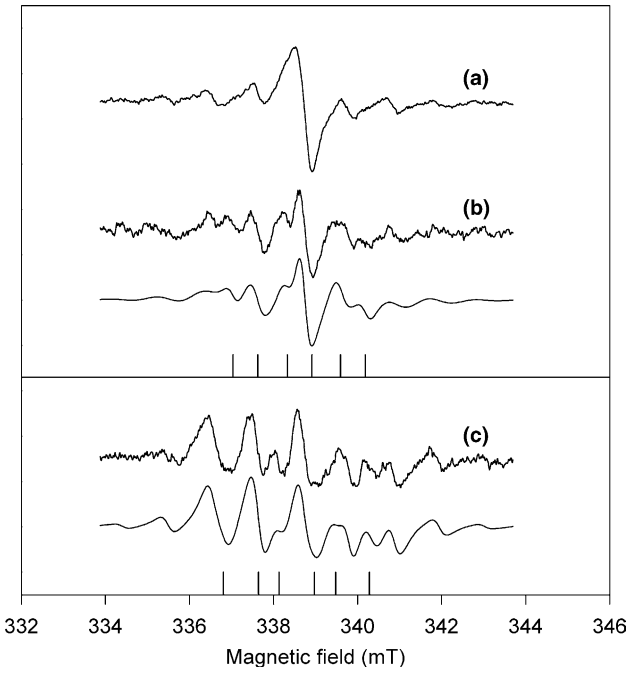

Fig. 4. OD ESR spectra of squalane solutions of: (a) 8×10^{-5} M *p*-TP + 2.5×10^{-3} M durene at $T = 259$ K; (b) 8×10^{-5} M *p*-TP + 2.5×10^{-3} M durene + 5×10^{-3} M TMPO at $T = 256$ K; (c) 8×10^{-5} M *p*-TP + 10^{-2} M durene + 10^{-2} M PMIO at $T = 250$ K. Smooth curves are modelling of the spectra with parameters: $a_H(4CH_3) = 1.07$ mT for durene RC; $a_N(NO) = 1.23$ mT, $a_H(CH) = 0.55$ mT for TMPO RA; $a_N(NO) = 1.34$ mT, $a_H(CH) = 0.94$ mT for PMIO RA, the individual line width is 0.27 mT.

Spectrum (a) is the spectrum of the squalane solution of 10^{-2} M deuterotoluene + 8×10^{-5} M *p*-TP + 10^{-2} M TMPO which consists of signals of deuterotoluene RC and TMPO RA. The hfc and *g*-values for the TMPO RA obtained by spectrum simulation (smooth curve under the spectrum (a)) are close to those obtained in experiments with TMPD. The integral intensities of the $TMPO^{\cdot -}$ and $(deuterotoluene)^{\cdot +}$ spectra are equal within the experimental accuracy.

In a similar experiment on PMIO, spectrum (b) has six lines whose positions correspond to the values $g = 2.0037 \pm 0.0001$, $a_N(NO) = 1.32$ mT, and $a_H(CH) = 0.90$ mT. As in the previous case, the integral intensities of signals of deuterotoluene RC and PMIO RA are equal.

3.3. Durene as a hole trap

Fig. 4 shows the OD ESR spectra of the squalane solution of 2.5×10^{-3} M durene + 8×10^{-5} M *p*-TP, and the same solution with TMPO or PMIO added. Spectrum (a) is the superposition of the durene RC multiplet with hfc $a_H(4CH_3) = 1.07$ mT [32] and the singlet of *p*-TP RA. Simulation indicates almost equal integral intensity of these contributions. Thus, the main contribution to this spectrum is made by the $(durene)^{\cdot +}/p\text{-}TP^{\cdot -}$ pairs.

Adding TMPO (spectrum (b)) or PMIO (spectrum (c)) to the solution leads to appearance of new lines corresponding to cyclic nitrone RAs. The spectra of *p*-TP radical ions give a relatively small contribution to the integral intensity. Therefore, the spectra are mainly formed by the equal contributions of the durene RC and RA of either TMPO or PMIO. The hfc values of nitrone RAs obtained by fitting of these spectra (smooth curves) are very close to those provided by previous experiments.

The averaged hfc constants for RAs of TMPO and PMIO are presented in Table 2.

3.4. Quantum chemical calculations

Analysis of the literature indicates that the DFT methods, especially with hybrid functionals, are the most successful in predicting hfc values of radicals and ion-radicals [29,33]. In this Letter, we applied B3LYP method, particularly recommended for hfc calculations [33].

It is well known that five-membered cyclic neutral nitroxide radicals have planar structure [29]. Nevertheless, according to our UB3LYP/6-311G** calculation, a five-membered ring of RAs is substantially bent. For example, the atoms C(3)C(4)C(5)N of the TMPO RA

Table 2
Experimental and calculated hfc constants (mT)

Radical anion	Method of geometry optimization	UB3LYP/6-311G**		UMP2/6-311G**		UPM3	Experiment
	Basis set	6-31G*(solvent)[a]	EPR-II	6-31G*	EPR-II	6-31G*	
PMIO$^{\cdot-}$	a_N(NO)	1.19 (1.21)	1.05	1.29	1.14	2.05	1.33 ± 0.03
	a_N(NCH$_3$)	0.006 (0.004)	0.005	0.016	0.017	−0.012	–
	a_H(CH)	0.90 (0.95)	1.27	0.94	1.31	−1.23	0.92 ± 0.04
	a_H(N-CH$_3$)	−0.006 (−0.008)	−0.008	−0.004	−0.007	0.005	–
	a_H (4C-CH$_3$)[b]	0.1, 0.002, 0.03, 0.03	⩽ 0.09	⩽ 0.08	⩽ 0.07	⩽ 0.18	–
	S^2	0.754 (0.754)	0.754	0.754	0.754	0.754	–
	S^2 (an)	0.750 (0.750)	0.750	0.750	0.750	0.750	–
TMPO$^{\cdot-}$	a_N(NO)	1.24 (1.26)	1.08	1.33	1.18	0.95	1.22 ± 0.03
	a_H(CH)	0.58 (0.62)	0.94	0.67	1.02	−1.24	0.51 ± 0.05
	a_H(CH$_2$)	−0.05 (−0.05)	−0.045	−0.05	−0.042	−0.052	–
	a_H (4CH$_3$)[b]	0.005, −0.03, −0.01, 0.08	⩽ 0.07	⩽ 0.05	⩽ 0.08	⩽ 0.19	–
	S^2	0.754 (0.754)	0.754	0.754	0.754	0.754	–
	S^2 (an)	0.750 (0.750)	0.750	0.750	0.750	0.750	–

Calculations are performed by the UB3LYP method with two basis sets for geometries optimised by UB3LYP, UMP2 and UPM3 methods, respectively. The calculated values of S^2 and the values after annihilation are also presented.

[a] Results of calculation in heptane obtained using PCM model.

[b] For every methyl group the calculated hfc constants were averaged to account for their free rotation.

lie almost in the plane. However, the C(2) atom stands out of this plane by 24.3°. The H—C(2) bond bents from the C(2)NO plane by 42.8°. It is known that geometrical factors significantly affect the hfc values. To confirm the non-planar structure, we also optimized the geometry of TMPO and PMIO RAs by UMP2/6-311G** method. It was found that geometries optimized by UMP2 method were very similar to those found by UB3LYP.

According to the calculations, the spin density in both RAs is localized mainly in the CNO fragment (0.39, 0.36, and 0.2, respectively, for both TMPO and PMIO at UB3LYP/6-31G* level). Table 2 summarizes the values for isotropic hfc constants of RAs predicted by UB3LYP calculations with two different basis sets and geometries optimized by the two different methods. Since geometries optimized by the two methods are similar, values of hfc calculated for these geometries are very close, too. Table 2 demonstrates that the hfc calculated with simple 6-31G* basis set are in a very good agreement with experiment, while results of calculations with a special EPR-II basis set deviate from experiment and the agreement is only qualitative.

Note, that the hfc constant a_H(CH) with the hydrogen atom, which bents significantly from the C=N—O plane, is positive and it is higher for PMIO RA due to the larger dihedral angle of this hydrogen with C=N—O plane (47.6°) comparing to TMPO (42.8°).

In contrast to the DFT and the MP2 methods, the semi-empirical PM3 calculation leads to an almost planar structure of the five-membered ring of RAs and thus, to a negative value of the hfc with the hydrogen atom bound to carbon atom of C=N—O fragment. Therefore, the procedure often used to calculate hfc constants and involving the optimization of the geometry at semi-empirical level (AM1 or PM3) followed by calculations of hfc constants using the INDO method fails for the case of nitrone RAs.

Thus, for both radical anions the predicted values of hfc constants a_N(NO) and a_H(CH) are in a good agreement with experiment. Other hfc constants are small and cannot be obtained under the experimental conditions we used.

4. Conclusion

It was demonstrated that the OD ESR method can be used to detect the short-lived radical anions of the cyclic nitrones (TMPO and PMIO) formed by radiolysis of their squalane solutions. The hfc constants of the RAs of both nitrones were determined experimentally and were found to be in quantitative agreement with the results of B3LYP/6-31G* calculations. Therefore, we can conclude from the calculations that RAs of five-membered cyclic nitrones have non-planar geometry with pyramidal NO moiety, and that the spin density in these RAs is localized in the C=N—O fragment.

Our data are indicative of an effective formation of the radical anions of cyclic nitrones upon radiolysis, which should be taken into account when using these compounds as spin traps.

Acknowledgements

The work was supported by the Russian Foundation for Basic Research (Grant No. 02-03-32224a), the program 'Leading Science Schools' (Grant No. 84.2003.3) and INTAS (Grant No. 00-0093).

References

[1] A.E. Favier, J. Cadet, B. Kalyanaraman, M. Fontecave, J.-L. Pierre (Eds.), Analysis of Free Radicals in Biological Systems, Birkhäuser Verlag, Basel, 1995.
[2] H. Chandra, M.C.R. Symons, J. Chem. Soc., Chem. Commun. (1986) 1302.
[3] V. Zubarev, O. Brede, J. Chem. Soc., Perkin Trans. 2 (1994) 1821.
[4] S. Bhattacharjee, M.N. Khan, H. Chandra, M.C.R. Symons, J. Chem. Soc., Perkin Trans. 2 (1996) 2631.
[5] L. Eberson, O. Persson, J. Chem. Soc., Perkin Trans. 2 (1997) 1689.
[6] L. Eberson, J. Chem. Soc., Perkin Trans. 2 (1992) 1807.
[7] A.R. Forrester, S.P. Hepburn, J. Chem. Soc. C (1971) 701.
[8] F.P. Sargent, E.M. Gardy, Can. J. Chem. 54 (1976) 275.
[9] V. Zubarev, R. Mehnert, O. Brede, Radiat. Phys. Chem. 39 (1992) 281.
[10] V. Zubarev, O. Brede, Radiat. Phys. Chem. 47 (1996) 365.
[11] L. Eberson, M.P. Hartshorn, O. Persson, J. Chem. Soc., Perkin Trans. 2 (1997) 195.
[12] J.-L. Clement, B.C. Gilbert, F.H. Win, N.D. Jackson, M.S. Newton, S. Silvester, G.S. Timmins, P. Tordo, A.C. Whitwood, J. Chem. Soc., Perkin Trans. 2 (1998) 1715.
[13] I.G. Kursakina, V.F. Starichenko, I.A. Kiriljuk, I.A. Grigor'ev, L.B. Volodarsky, Izv. Akad. Nauk. SSSR, Ser. Khim. 9 (1991) 2009 (in Russian).
[14] L. Eberson, O. Persson, J. Chem. Soc., Perkin Trans. 2 (1997) 893.
[15] L.A. Shundrin, V.A. Reznikov, I.G. Irtegova, V.F. Starichenko, Izv. Akad. Nauk., Ser. Khim. 4 (2003) 892 (in Russian).
[16] Y.N. Molin, O.A. Anisimov, V.I. Melekhov, S.N. Smirnov, Faraday Discuss. Chem. Soc. 78 (1984) 289.
[17] Y.N. Molin, O.A. Anisimov, Radiat. Phys. Chem. 21 (1983) 77.
[18] H. Fischer, K.-H. Hellwege (Eds.), Landolt-Börnstein. Numerical Data and Functional Relationships in Science and Technology, N.S., GroupII, V.9: Magnetic Properties of Free Radicals, Part d1, Springer-Verlag, Berlin, 1980.
[19] I.A. Grigor'ev, G.I. Schukin, V.V. Martin, V.I. Mamatyuk, Chem. Heterocycl. Compd. Engl. Transl. 21 (1985) 210.
[20] L. Wojnarovits, G. Foldiak, J. Chromatogr. Sci. 206 (1981) 511.
[21] C. Santiago, R.W. Gandour, K.N. Houk, W. Nutakul, W.E. Cravey, R.P. Thummel, J. Am. Chem. Soc. 100 (1978) 3730.
[22] K.-T. Lu, G.C. Eiden, J.C. Weisshaar, J. Phys. Chem. 96 (1992) 9742.
[23] R. Egdell, J.C. Green, C.N.R. Rao, Chem. Phys. Lett. 33 (1975) 600.
[24] J.J.P. Srewart, J. Comput. Chem. 10 (1989) 221.
[25] A.D. Becke, J. Chem. Phys. 98 (1993) 5648.
[26] C. Lee, W. Yang, R.G. Parr, Phys. Rev. B 37 (1988) 785.
[27] M.J. Frisch et al., GAUSSIAN 98, Revision A.6, Gaussian Inc., Pittsburgh, PA, 1998.
[28] C. Adamo, V. Barone, A. Fortunelly, J. Chem. Phys. 102 (1995) 384.
[29] R. Importa, V. Barone, Chem. Rev. 104 (2004) 1231.
[30] S. Miertus, E. Scrocco, J. Tomasi, Chem. Phys. 55 (1981) 117.
[31] M. Cossi, V. Barone, R. Cammi, J. Tomasi, Chem. Phys. Lett. 255 (1996) 327.
[32] H. Fischer, K.-H. Hellwege (Eds.), Landolt-Börnstein. Numerical Data and Functional Relationships in Science and Technology, N.S., GroupII, V.9: Magnetic Properties of Free Radicals, Part d2, Springer-Verlag, Berlin, 1980.
[33] T. Bally, W.T. Borden, in: K.B. Lipkowitz, D.B. Boyd (Eds.), Rev. Comp. Chem., vol. 13, Wiley–VCH, New York, 1999, p. 1.